

# Nondestructive analysis of senescence in mesophyll cells by spectral resolution of protein synthesis-dependent pigment metabolism

Alan Gay<sup>1</sup>, Howard Thomas<sup>2</sup>, María Roca<sup>3</sup>, Caron James<sup>1</sup>, Janet Taylor<sup>1</sup>, Jem Rowland<sup>4</sup> and Helen Ougham<sup>1</sup>

<sup>1</sup>Institute of Grassland and Environmental Research, Plas Gogerddan, Aberystwyth, Ceredigion SY23 3EB, UK; <sup>2</sup>Institute of Biological Sciences, Aberystwyth University, Ceredigion SY23 3DA, UK; <sup>3</sup>Instituto de la Grasa (CSIC), Avda Padre García Tejero 4, Sevilla 41012, Spain;

<sup>4</sup>Department of Computer Science, Aberystwyth University, Ceredigion SY23 3DB, UK

## Summary

Author for correspondence:

Helen Ougham

Tel: +44 (0)1970 823094

Fax: +44 (0)1970 823242

Email: helen.ougham@bbsrc.ac.uk

Received: 16 November 2007

Accepted: 15 January 2008

- Over 6 d of dark-induced senescence, leaf segments of wild-type *Lolium temulentum* lost > 96% chlorophyll *a + b*; leaves from plants containing a staygreen mutation introgressed from *Festuca pratensis*, which has a lesion in the senescence-associated fragmentation of pigment-proteolipid complexes, retained over 43% of total chlorophyll over the same period.
- Mutant segments preferentially retained thylakoid membrane proteins (exemplified by LHCP II) but lost other cellular proteins at the same rate as wild-type tissue. The protein synthesis inhibitor D-MDMP inhibited chlorophyll degradation and partially prevented protein loss in both genotypes, but tissues treated with the ineffective L-stereoisomer were indistinguishable from water controls.
- Principal-components analysis of leaf reflectance spectra distinguished between genotypes, time points and D-MDMP treatments, showing the disruption of pigment metabolism during senescence brought about by the staygreen mutation, by inhibition of protein synthesis and by combinations of the two factors.
- The build-up of oxidized, dephosphorylated and phaeo-derivatives of chl *a* during senescence of staygreen tissue was prevented by D-MDMP and associated with characteristic difference spectra when senescent mutant tissue was compared with wild-type or inhibitor-treated samples. The suitability of senescence as a subject for systems biology approaches is discussed.

**Key words:** chlorophyll, chloroplast, MDMP, multivariate analysis, mutant, senescence, Systems Biology.

*New Phytologist* (2008) **179**: 663–674

© The Authors (2008). Journal compilation © *New Phytologist* (2008)

doi: 10.1111/j.1469-8137.2008.02412.x

## Introduction

In this paper we describe how genetic and chemical interference with the progress of leaf senescence alters the pathway of chlorophyll catabolism and may be observed noninvasively by spectral reflectance and chemometrics. During mesophyll senescence, chloroplasts transdifferentiate into gerontoplasts, a type of organelle which should be considered not as damaged or disorganized, but as a developmental stage in the plastid life cycle (Thomas *et al.*, 2003). Diagnostic of the chloroplast-

to-gerontoplast transition is induction of the pathway of chlorophyll (chl) catabolism (Thomas *et al.*, 2001; Ougham *et al.*, in press). Most of the enzymes and corresponding genes for chlorophyll catabolism have been identified in recent years (Kräutler & Hörtensteiner, 2006; Tanaka & Tanaka, 2006; Ougham *et al.*, in press). This pathway is sensitive to interruption by genetic mutation and chemical treatments (Thomas & Howarth, 2000; Ougham *et al.*, in press). Previously we described the introgression of a mutant (staygreen) allele into *Lolium temulentum* L. from *Festuca pratensis* Huds. (Thomas

*et al.*, 1999). Opening of the tetrapyrrole macrocycle is disabled in staygreen mutants of this type and hence they retain the majority of their chl during senescence (Roca *et al.*, 2004). It has long been known that senescence is also sensitive to inhibitors of gene expression, particularly chemicals that disrupt protein synthesis on cytoplasmic ribosomes (Thomas & Stoddart, 1980). In the present study, we used MDMP, a stereospecific inhibitor of eukaryotic translation (Baxter *et al.*, 1973) and leaf senescence (Thomas, 1976).

Introducing blockages into the chl breakdown pathway causes characteristic changes in the pools of upstream intermediates (Roca *et al.*, 2004; Ougham *et al.*, in press), which in turn would be expected to change the spectral properties of the tissue. There is an extensive literature on the reflectance properties of leaves, much of it relating to large-scale remote sensing of vegetation (Merzlyak *et al.*, 1999; Richardson *et al.*, 2002; Sims & Gamon, 2002; Zarco-Tejada *et al.*, 2005). To observe and classify subtle compositional changes resulting from genetic or chemical interruption of chlorophyll degradation, we used a combination of spectral data collection and chemometric analysis.

Spectral data sets can be highly informative of the state of the object, but are usually very large and need to be analysed by the appropriate multivariate and machine-learning methods to extract meaningful information from them and to take account of features such as multicollinearity (Mitchell, 1997; Manly, 2000; Naes *et al.*, 2004; Witten & Frank, 2005; Bishop, 2006). In the present study, we analyse the compositional consequences for *L. temulentum* senescence of introducing a staygreen mutation or MDMP treatment, or both, and relate these to the spectral properties of leaf tissue determined nondestructively and analysed by multivariate methods.

## Materials and Methods

### Plant material

Wild-type (Y) and staygreen (G) lines of *Lolium temulentum* Ceres, near isogenic for an introgression from a senescence mutant of *Festuca pratensis*, were generated as described by Thomas *et al.* (1999). Plants were grown from seed on vermiculite, seven plants per 5 inch pot, in a controlled environment providing a constant 20°C and 8 : 16 h light : dark cycle (light flux 350  $\mu\text{mol m}^{-2} \text{s}^{-1}$ ). Plants were fed with a nutrient solution as described by Gay & Hauck (1994).

### Treatments

Tissue was harvested from the fully expanded youngest (fourth) leaf 5–6 wk after seed sowing. Laminae were cut into 3 cm lengths and surface-sterilized by immersion for 5 min in 1.2% sodium hypochlorite solution containing four drops of Tween 20 per 250 ml followed by thorough rinsing with five changes of sterile water. Segments were incubated under aseptic conditions at 20°C in continuous darkness by floating

them lower side down on water, 10  $\mu\text{M}$  L-MDMP or 10  $\mu\text{M}$  D-MDMP in 9-cm-diameter Petri dishes (usually seven segments per dish). The stereoisomers of MDMP (2-(4-methyl-2,6-dinitroanilino)-*N*-methyl-propionamide; Baxter *et al.*, 1973) were chemically synthesized by Dr Richard Simmonds, Aberystwyth University. Freshly harvested tissue was used for 0 d samples. At 2, 4 and 6 d, control and MDMP-treated segments were rinsed with distilled water and, to avoid contributions from injured cells at cut surfaces, 2–3 mm of tissue at each end of each segment was discarded. Leaf segments were scanned for reflectance spectra as described in the following sections. Tissue for extraction was weighed, immediately frozen in liquid N<sub>2</sub> and stored at –80°C for later analysis.

### Recording and multivariate analysis of spectral data

Optical reflectance spectra of the leaf samples were obtained using an ImSpector direct sight imaging spectrograph (Spectral Imaging Ltd, Oulu, Finland). This is a passive optical device that, when interposed between a camera and a lens, permits acquisition of an individual spectrum at pixel resolution along a linear slice through the field of view. This results in an image in which the horizontal axis represents displacement along that line and the vertical axis corresponds to wavelength; each pixel in this image therefore represents the reflected intensity at a specific wavelength at a specific location on a line across the current sample. The ImSpector used was type V9, which has a nominal spectral range of 430–900 nm but this is subject to modification by the spectral characteristics of the camera used and the geometry of the ImSpector/camera combination.

For the present study, the ImSpector was attached to the C-mount of a Hitachi KP-M1EK monochrome CCD video camera with AGC (automatic gain control) disabled and gamma correction set to 1.0. The optical IR-cut filter fitted in front of the CCD in the camera was removed and this extended the spectral response from the normal cutoff of 700 nm towards the infrared. Wavelength calibration of the ImSpector/camera combination was effected with a mercury vapour lamp, aided by coloured LEDs to resolve possible ambiguity in identifying the mercury lines. This revealed that the effective spectral range was approx. 461–854 nm. A linear least-squares fit was applied to the relationship between pixel number on the spectral axis and mercury line wavelength ( $r^2 = 0.999$ , with no improvement using a quadratic fit). This was used to provide the following empirical wavelength calibration, where wavelength is in nm and 'pixel' refers to pixel number on the spectral axis in the range 1–260:

$$\text{Wavelength} = (\text{pixel} \times 1.51) + 461.65 \quad \text{Eqn 1}$$

Image capture was via a desktop personal computer fitted with a low-cost video capture card. Illumination was by means of two 12 V quartz-halogen lamps. Acquired images were in the form of raw binary files that were unpacked by means of

a simple Perl script to provide ASCII decimal image files of 760 pixels in the spatial dimension and 260 pixels along the spectral axis. Lens aperture, exposure time and lighting were all kept constant throughout and data were recorded with nominal 8 bit intensity resolution, but maximum values were restricted to 7 bit resolution to avoid any possibility of saturation. Initial checks were made for the presence of any anomalous extra bright pixels in the leaf regions of the images (see later for definition) by calculating the ratio of mean to median reflectance, and as this only varied between 0.95 and 1.01, the absence of extra-bright pixels was confirmed.

Initial observations showed that there was a slight difference in illumination across the field of view ( $\pm 1\%$ ), so to reduce systematic bias an average was taken over the illuminated leaf surface at each wavelength, containing 200 separate pixels on the spatial axis from the same part of the field of view for each sample. The ratio of the leaf value to that of the mean of two 60-pixel-wide regions on the spatial axis of the background paper on either side of the leaf (taken far enough away from the leaf to avoid direct shadows, and from fixed regions in the field of view) was then calculated, thus ensuring that the comparison between samples was unaffected by the slightly uneven illumination. Values were finally corrected to a known reflectance of substandard (Spectralon<sup>®</sup>, Labsphere Inc., North Sutton, NH, USA), which had previously been compared with the background paper. This procedure also accounted for the changes in the relative sensitivity of the ImSpector/camera combination with wavelength. For each group of five leaves, single spectra were produced for their upper and lower surfaces, and named according to genotype, days of senescence, chemical treatment and whether the upper or lower leaf surface was scanned. For tissue incubated on water or MDMP for 2, 4, 6 and 8 d, this gave four time points  $\times$  two surfaces  $\times$  two genotypes  $\times$  two treatments = 32 data objects. For 0 d (unsenesced) tissue, observations were made on two surfaces  $\times$  two genotypes = four data objects, making a total of 36 data objects, each with 260 spectral variables.

To investigate whether the spectra were able to distinguish the different groups, principal-components analysis (PCA, Hotelling, 1933) was applied to the set of 36 spectra, after scaling values at each wavelength to zero mean and unit variance, using MATLAB 7 (The MathWorks Ltd, Natick, MA, USA). The first six principal components were found to account for 70.36, 10.77, 5.45, 2.72, 1.54 and 1.34%, respectively, of the variance in the data.

Leaf colour was quantified by pixel analysis of high-resolution JPEG images of leaf segments. RGB (red-green-blue) profiles across a montage of segments were obtained using the 'improfile' tool in MATLAB.

### Protein extraction and electrophoresis

Frozen leaf material was ground to a fine powder with liquid N<sub>2</sub> and sand, in a mortar and pestle. The powder was

homogenized with 5 ml g<sup>-1</sup> FW extraction buffer (EB) comprising 0.2 mM tris, pH 8.0, containing 5% (v/v) glycerol, 1% (v/v) 2-mercaptoethanol, 1 mM PMSF and 1 mM monoiodoacetate, and allowed to thaw before adding 20% (w/v) lithium dodecyl sulphate (LiDS; 0.5 ml g<sup>-1</sup> FW) and homogenizing further. The homogenate was heat-denatured by boiling for 2 min, cooled and centrifuged at 12 500 g<sub>av</sub> for 10 min. Protein in the supernatant was determined according to Lowry *et al.* (1951). Total LiDS-EB-extracted proteins were fractionated by 12.5% SDS polyacrylamide gel electrophoresis (SDS-PAGE; Laemmli, 1970) using a Bio-Rad mini-gel system. Aliquots of extracts were loaded on the basis of equal weight of leaf tissue. Gels were stained with Coomassie Brilliant Blue.

### High-performance liquid chromatography (HPLC) of leaf pigments

Leaf segments were frozen in liquid nitrogen and ground to a fine powder in a pestle and mortar with quartz sand. The pigments were extracted with 80% acetone (1.5 ml per 100 mg tissue) and, after centrifugation at 10 000 g<sub>av</sub> for 10 min at 4°C, chlorophylls and related pigments were determined by HPLC (Roca *et al.*, 2004). Pigments were identified from their spectral absorption maxima and peak ratios and by HPLC cochromatography with authentic samples. Identification of 13<sup>2</sup> hydroxy chlorophyllide *a* is tentative, based on spectral absorption maxima and peak ratios. Online UV-visible spectra were recorded from 350–700 nm with a photodiode array detector. HPLC was performed on a Nova-Pak C18 4  $\mu$ m Radial-Pak cartridge 8 mm  $\times$  100 mm column using Waters 515 HPLC pumps and a Waters model 996 photodiode array detector. The manual injection valve (Rheodyne, model 7725I) was fitted with a 20  $\mu$ l loop. Separation was carried out using an elution gradient (2 ml min<sup>-1</sup>) with the mobile phases (A) ion pair reagent/methanol (1 : 4 v/v) and (B) acetone/methanol (1 : 4 v/v). The ion pair reagent was 1 M ammonium acetate in water (Langmeier *et al.*, 1993). The gradient was isocratic A 4 min, A to B 5 min, isocratic B 9 min, return to A 2 min (Siefertmann-Harms, 1987), and detection was at 660 nm. Analytically pure samples of chl *a* and chl *b* were used to obtain the calibration slopes representing the area of the peak obtained with different injected volumes of pure solutions of known concentration. The same preparation was acidified and used for calibration with regard to phaeophorbides (phd). For quantification of chlorophyllides (chld) it was assumed that dephytylation does not change the spectral properties of the porphyrin moiety (Langmeier *et al.*, 1993).

## Results

### Senescence and its response to D- and L-MDMP

Retention of chl is an intrinsic character of the foliage of staygreen *L. temulentum* genotypes, expressed under every

**Table 1** Pigment contents of control and MDMP-treated *Lolium temulentum* leaf tissue

			Chl <i>a</i>	Chl <i>b</i>	Total chl	Chl <i>a</i> : <i>b</i>	Chld <i>a</i>	Chld <i>a</i> '	OH-chld <i>a</i>	OH-phd <i>a</i>	Phd <i>a</i>	Phd <i>a</i> '	
Y (wild-type)	0 d	C	480 ± 112	149 ± 39	629 ± 151	3.24 ± 0.10	0	0	0	0	0	0	
		D	415 ± 40	127 ± 13	542 ± 53	3.27 ± 0.08	0	0	0	0	0	0	
		L	511 ± 74	163 ± 28	674 ± 101	3.15 ± 0.13	0	0	0	0	0	0	
	4 d	C	424 ± 36	123 ± 33	553 ± 128	3.29 ± 0.03	0	0	0	0	0	0	
		D	202 ± 33	48 ± 8	251 ± 40	4.20 ± 0.35	0	0	0	0	0	0	
		L	399 ± 88	135 ± 27	543 ± 114	2.95 ± 0.08	0	0	0	0	0	0	
	6 d	C	181 ± 8	40 ± 2	222 ± 9	4.51 ± 0.21	0	0	0	0	0	0	
		D	17 ± 2	5 ± 2	22 ± 2	2.66 ± 0.75	0	0	0	0	0	0	
		L	398 ± 9	148 ± 23	546 ± 18	2.75 ± 0.51	0	0	0	0	0	0	
	G (staygreen)	0 d	C	628 ± 107	190 ± 12	817 ± 119	3.29 ± 0.36	0	0	0	0	0	0
			D	578 ± 83	175 ± 25	756 ± 108	3.31 ± 0.03	3 ± 2	0	0	0	0	0
			L	601 ± 106	188 ± 33	789 ± 139	3.20 ± 0.07	0	0	0	0	0	0
4 d		C	733 ± 81	221 ± 20	954 ± 100	3.32 ± 0.80	6 ± 0	0	0	0	0	0	
		D	461 ± 82	110 ± 11	632 ± 106	4.18 ± 0.36	46 ± 13	0	7 ± 3	0	9 ± 1	0	
		L	530 ± 45	161 ± 10	691 ± 54	3.29 ± 0.14	0	0	0	0	0	0	
6 d		C	523 ± 119	104 ± 23	693 ± 148	5.04 ± 0.30	50 ± 4	0	7 ± 1	0	9 ± 2	0	
		D	312 ± 50	63 ± 8	461 ± 49	4.92 ± 0.19	23 ± 3	3 ± 2	0	13 ± 2	43 ± 7	5 ± 2	
		L	587 ± 13	174 ± 8	761 ± 22	3.39 ± 0.18	0	0	0	0	0	0	
6 d		C	312 ± 45	57 ± 3	453 ± 60	5.49 ± 0.58	16 ± 5	0	0	11 ± 3	49 ± 5	5 ± 0	
		D											
		L											

Leaf tissue of wild-type and staygreen genotypes was incubated in darkness for up to 6 d on water (C), L-MDMP (L) or D-MDMP (D). Chlorophylls and related pigments were quantified by HPLC. Pigment contents given as  $\mu\text{g g}^{-1}$  FW  $\pm$  SD. The values represent the means of three determinations. Total chl, fraction comprises chlorophyll *a* and *b* plus phytylated and dephytylated chlorophylls; Chld, chlorophyllide; Phd, phaeophorbide; OH-chld, 13<sup>2</sup>-OH chlorophyllide *a*; OH-phd, 13<sup>2</sup>-OH phaeophorbide *a*; Chld *a*' and Phd *a*', 27-S-epimeric isomers of Chld *a* and Phd *a*, respectively.

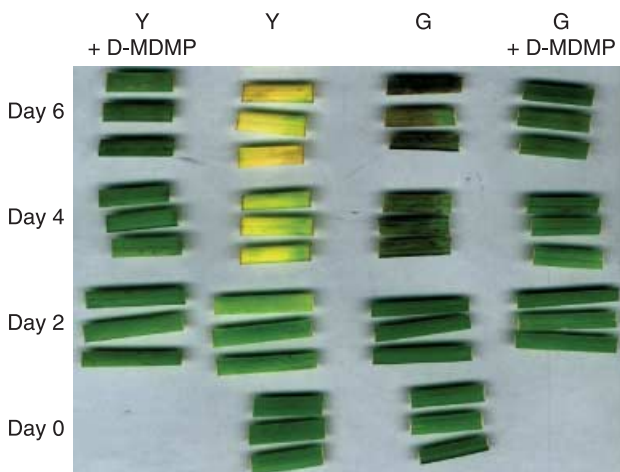


**Fig. 1** Excised leaf segments of *Lolium temulentum* Ceres wild-type (Y) and containing the introgressed staygreen mutation (G), incubated in darkness for 0, 2, 4 and 6 d in the absence (centre columns) or presence (outer columns) of the protein synthesis inhibitor D-MDMP.

circumstance that normally promotes physiological yellowing. When excised tissues were incubated on water in the dark, Y leaves had visibly begun to de-green after 2 d, and by 6 d were almost completely yellow (Fig. 1). Over the same timescale,

tissue of the line carrying the staygreen introgression remained green, although the eye was able to discern some fading and slight changes in leaf colour from bright to olive green. Leaf segments treated with L-MDMP had a similar appearance to those incubated on water; but the D-stereoisomer of MDMP which, unlike L-, is a potent inhibitor of cytosolic protein synthesis, prevented visible degreening in Y tissue. D-MDMP also inhibited the subtle pigmentation changes in G leaf segments.

#### Pigments in MDMP-treated tissue

Chlorophylls and related pigments were analysed by HPLC. Only chl *a* and chl *b* were detected in Y tissue at each time-point and treatment (Table 1, Fig. 2). In the G genotype, chld *a* appeared at day 2, increased further by day 4 and declined somewhat at day 6 (Table 1). From day 4 other chl derivatives began to appear, including allomers and hydroxylated forms of chld *a* and phd *a* (Fig. 2, Table 1). No derivatives of chl *b* were detected. The chl *a* : *b* ratio increased markedly during senescence of G tissue, whereas in Y leaves the ratio increased somewhat to day 4, then declined. D-MDMP treatment prevented any significant loss of chl from either genotype, blocked the formation of chlds and phaeo-pigments in the staygreen mutant (Fig. 2, Table 1) and inhibited the senescence-related increase in chl *a* : *b* ratio. In practically all cases, L-

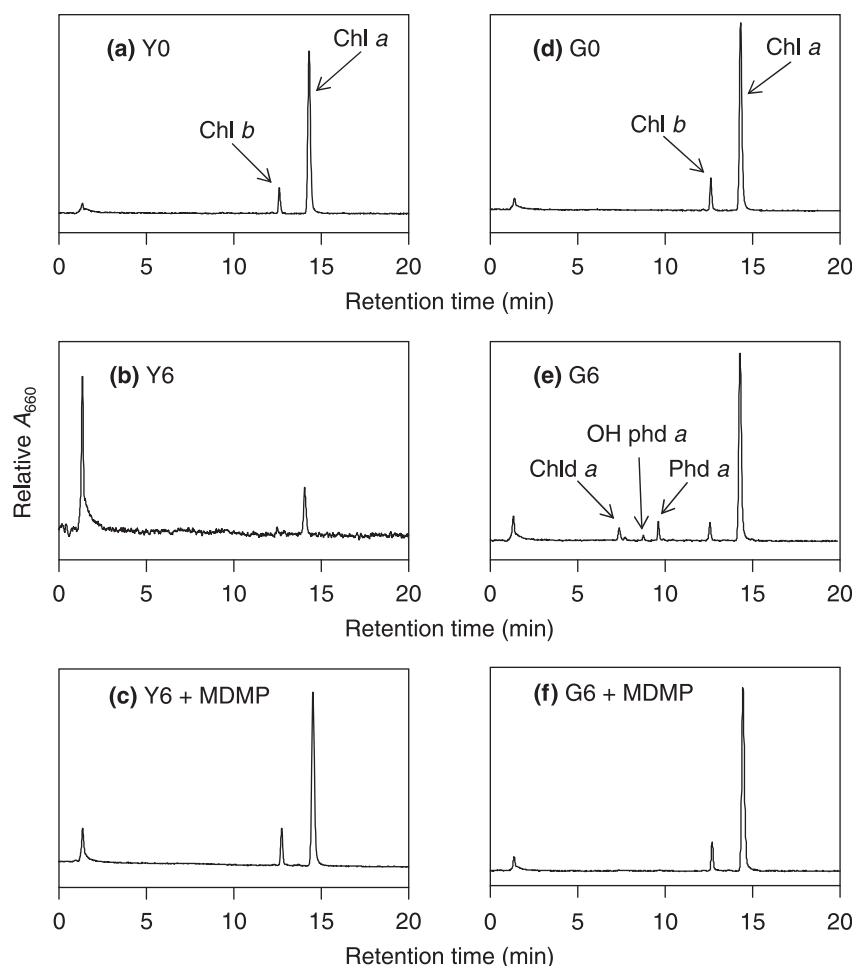


**Fig. 2** High-performance liquid chromatography chromatograms of chlorophylls and related pigments from *Lolium temulentum* leaf tissue during senescence. (a–c) Pigments from wild-type; (d–f) pigments from staygreen mutant. (a, d) 0 d of senescence; (b, e) control, 6 d of senescence; (c, f) D-MDMP-treated, 6 d of senescence. Chl, chlorophyll; phd, phaeophorbide; Chld, chlorophyllide; OH-phd a, 13<sup>2</sup>-OH phaeophorbide a.

MDMP-treated tissue was essentially identical to the water control (Table 1).

### Proteins in MDMP-treated tissue

Total protein was extracted from leaf segments by solubilization in hot detergent and analysed by SDS-polyacrylamide gel electrophoresis (Fig. 3). Over 6 d dark incubation, most of the protein was lost from tissues of both genotypes, but from 2 d onward, G segments retained significantly more protein than those of Y at each assay point. L-MDMP-treated tissues behaved like water controls (Fig. 3a,b). D-MDMP partially prevented protein loss from Y segments (Fig. 3a). In the G genotype, only at day 6 was protein content in D-MDMP-treated samples significantly higher than control and L-MDMP treatments (Fig. 3b).

The corresponding gel separations are presented in Fig. 3(c,d). Based on many previous studies of *Lolium* and *Festuca* leaf proteins, correlating total protein patterns with immunoblots, the identities of major components can be assigned. The most prominent polypeptide is a densely stained band at *c.* 50 kDa, corresponding to the large subunit of

rubisco. The rubisco small subunit, *c.* 18 kDa, is also abundant in 0 d samples. The light-harvesting proteins of photosystem II (LHCP II) are represented by a tight group of polypeptides at *c.* 24 kDa. The behaviour of rubisco and LHCP II is indicative of the general state of stroma and intrinsic thylakoid membrane proteins, respectively. In control and L-MDMP treatments of both genotypes, the staining intensity of the rubisco bands decreased in step with total protein. In both genotypes, rubisco subunits were relatively stable over 4 d of treatment with D-MDMP, but the staining intensity of the corresponding bands had decreased sharply by 6 d. D-MDMP also stabilized the amounts of a component of *c.* 65 kDa, running just above the rubisco large subunit. LHCP II polypeptides were appreciably less labile in control and L-MDMP-treated G than in wild-type samples. D-MDMP almost completely inhibited loss of LHCP II.

### Discrimination between genotypes and treatments by PCA

Reflectance spectra in the range 450–850 nm at each point along a selected leaf segment were captured using an ImSpector

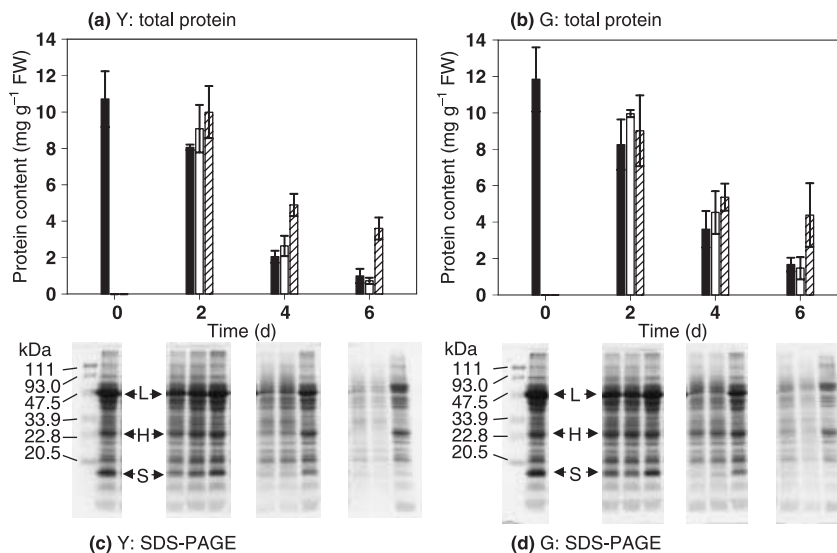


**Fig. 3** Changes in protein contents of excised leaf segments during senescence in the dark. (a, c) Wild-type *Lolium temulentum* Ceres; (b, d) homozygous for the staygreen mutation. (a, b) Closed columns, controls; open columns, treated with L-MDMP; hatched columns, treated with D-MDMP. Values represent the means of three determinations with error bars showing SD. (c, d) Molecular weight standards are shown on the left. L and S, large and small subunits of Rubisco, respectively; H, the position of the LHCPII band.

imaging spectrograph run from a desktop computer. Data were averaged and subjected to PCA. Discrimination between genotypes and incubation times was achieved by plotting the first two principal components (Fig. 4). In each case, spectra from the upper and lower surfaces of the same sample were highly similar, effectively behaving as replicates and demonstrating the reproducibility of the data. The time series for each genotype described a trajectory through PC space (indicated by arrows in Fig. 4a). Tissue of both genotypes at 0 d clustered in the region of the plot defined by a PC1 score of between  $-5$  and  $-10$  and a PC2 value  $c. -5$ . As Y tissue senesced, the PC1 score markedly increased towards 30, whereas PC2 increased by only a small amount. By contrast, senescence of tissue of the G mutant between 0 and 6 d was associated with a large increase in PC2 value and a relatively small decrease in PC1. Between 6 and 8 d there was a decrease in PC2 score and an increase in PC1.

Figure 5 shows the eigenvector coefficients (the weighting multipliers applied to the individual wavelength values before summation over all wavelengths to give a principal component value for a sample) for PC1, PC2 and PC3, which account for  $> 85\%$  of data variance. The weightings for PC1 largely contrast the reflectance in the 500–720 nm range (the blue-green through to the red part of the spectrum) with that below 500 nm (blue) and over 740 nm (near infra red). PC2 generally weights reflectance positively over all wavelengths, but with a negative contribution between 720 and 740 nm, which is coincident with the red edge where reflectance is changing rapidly between low values in the visible region and high values in the near-infrared. PC3 positively weights reflectances below 560 nm (the green and blue end of the spectrum) and provides almost a mirror image of the weightings of PC2 near to the red edge, whilst giving negative weights in other spectral regions. This complex combination of both narrow and wide bands within the principal components demonstrates the

importance of collecting well resolved spectral information to discriminate between the wild-type, mutant and inhibitor-treated leaves.

#### Inhibiting protein synthesis 'freezes' tissue in the presenescent state

Treatment of Y and G tissue with D-MDMP strongly interfered with the trajectories in the PCA plot (Fig. 4b). D-MDMP-treated samples clustered in the region of control 0 and 2 d samples, although by 6 d D-MDMP-exposed tissues of both genotypes had become slightly separated from the remainder. Difference reflectance spectra were generated between combinations of time-points, treatments and genotypes. A set of difference spectra is presented in Fig. 6(a), illustrating the similarity between the 6 d D-MDMP samples and the 0 d samples, as indicated by the Y6M minus Y0 line. Accordingly, the difference spectrum for Y control at day 6 compared with Y at day 0 was practically identical to that of Y day 6 control against day 6 D-MDMP-treated. The strong double peak at 645 and 680 nm observed when comparing 6 d senesced Y leaves with unsenesced or D-MDMP-treated Y leaves primarily represents the loss of chl *a* and *b*. D-MDMP blocked all the spectral changes associated with senescence, illustrating the dependence of the earlier steps in chl degradation on protein synthesis.

#### Relating difference spectra to pigment composition in senescing tissue

Figure 6(b) presents a comparison between 6 d senesced and unsenesced G leaves. The difference spectra for upper and lower surfaces were virtually identical. Reflectance at 580–650 nm increased between day 0 and day 6, whereas there was a decrease at  $c. 700$  nm. Phaeophorbide *a* is the major compound derived, but spectrally different, from chl upstream

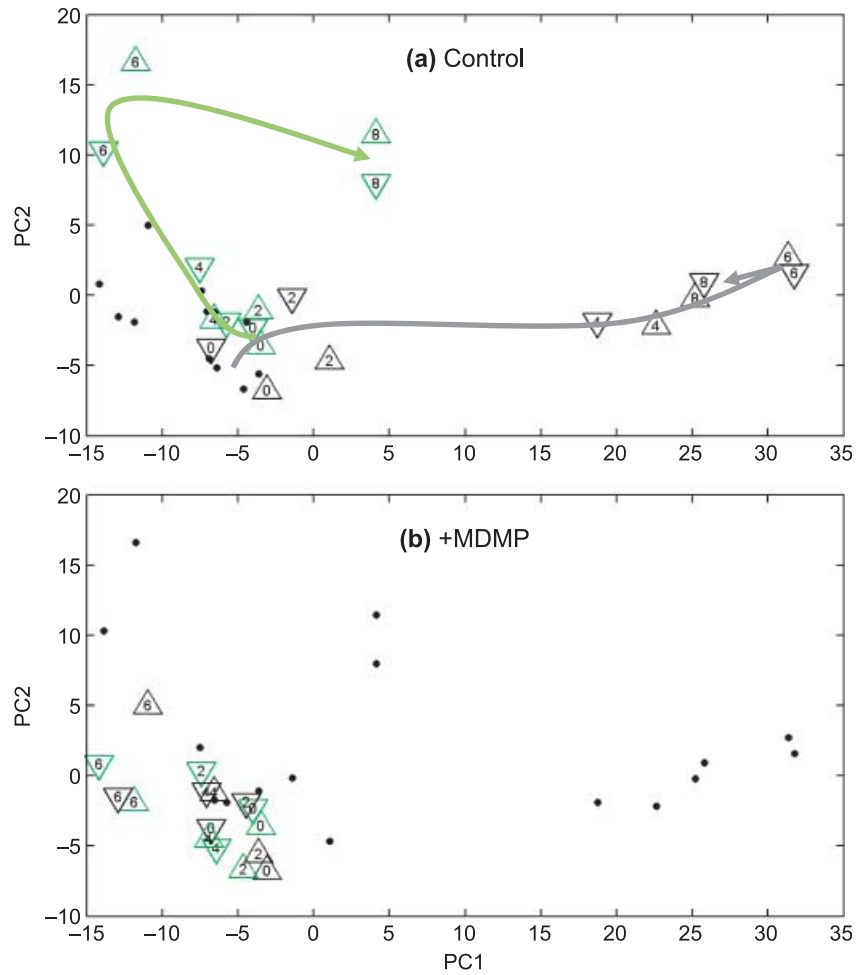


**Fig. 4** Principal-components analysis (PCA) plot of spectral analyses of senescing *Lolium temulentum* leaf segments. (a) Control treatment data (triangles); data from MDMP treatment (dots). (b) D-MDMP treatment data (triangles); control data (dots). The first two principal components (PC1 and PC2) accounted for 81% of the sample variation. Sample codes: triangles, apex up, upper leaf surface scanned; triangles, apex down, lower surface; digit in plotting symbol, days of senescence; green and black symbols, genotypes G and Y, respectively.

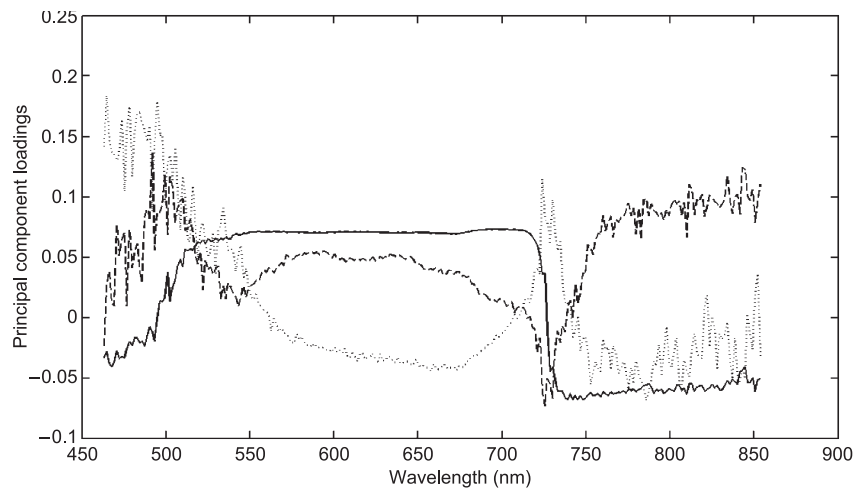


**Fig. 5** Vector plot of the first three principal components from principal-components analysis (PCA) of leaf spectra. Eigenvectors for PC1 and PC2 show wavelengths at which discrimination between leaf samples is highest. All nonzero values, irrespective of sign, indicate a contribution to the analysis. PC1, solid line; PC2, dashed line; PC3, dotted line.

of the metabolic blockage in G leaves (Table 1); the absorption spectrum of phd *a* was obtained from the HPLC photodiode array data and plotted after first inverting by multiplying by  $-1$  (Fig. 6b). It is noticeable that the phd spectrum in the 550–650 nm region resembles the reflectance difference

plot quite closely, but is blue-shifted by *c.* 10–15 nm (phd peaks at 586 and 621 nm, difference spectrum peaks 594 and 635 nm, respectively).

The G day 6 minus G day 0 difference plot in Fig. 6(b) indicates a marked change in the balance between reflectance

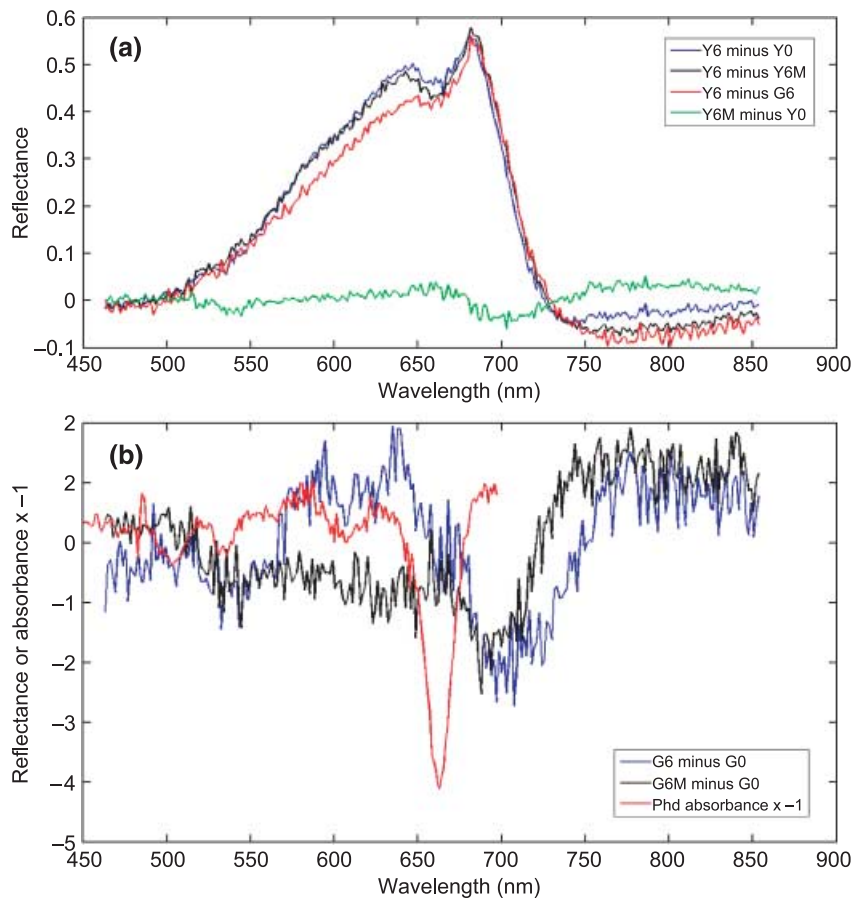


**Fig. 6** Difference plots demonstrating spectral differences between genotypes and MDMP treatments in *Lolium temulentum* leaf segments at 6 d of senescence. (a) Wild-type control or D-MDMP treatment at day 6 (Y6 and Y6M, respectively) compared with Y at day 0 (Y0) and staygreen control at day 6 (G6). (b) G day 6 control and D-MDMP-treated (G6 and G6M, respectively) compared with G at day 0. The absorbance spectrum of phaeophorbide *a*, from high-performance liquid chromatography photodiode array detection, is also plotted, inverted by multiplying values by  $-1$ . All leaf data are from scans of the upper surface of the tissue; spectra from the corresponding lower surfaces were essentially identical. Data are plotted after autoscaling (ordinate values are arbitrary). The reflectance data from which the difference spectra in Fig. 6(b) were derived are presented in the Supplementary material (Fig. S1).

in the green and red regions of the spectrum. To visualize this, we carried out an analysis of relative RGB values of pixels in JPEG images of leaf segments (Fig. 1). Figure 7 presents the results of scans across groups of G segments arranged by replicate (three per time point), days of senescence and control or D-MDMP treatment. It is clear that the intensity of green relative to red decreased markedly between 0 and 6 d in control tissue. The convergence of red and green values was completely prevented by D-MDMP treatment over the same timescale.

## Discussion

### Differential sensitivities to MDMP of components of the senescence syndrome

Previous publications on *Brassica rapa* (Ginsburg & Matile, 1993) and *L. temulentum* (Roca *et al.*, 2004) have shown that the mechanism of chl catabolism and chl-associated protein degradation during senescence of isolated leaf tissue is essentially identical to that of intact leaves. Accordingly, from comparisons of pigment metabolism in leaf segments of G and Y *L. temulentum*, the process of chlorophyll and pigment-protein breakdown in all modes of leaf senescence may be inferred.

This approach has been employed to separate out those parts of the senescence syndrome that require new proteins to be made. MDMP was originally synthesized at Shell Research Ltd as a putative herbicide. Baxter *et al.* (1973) reported that it is a potent inhibitor of the function of 80S (cytosolic) ribosomes. Thomas (1976) showed that the D-stereoisomer blocked protein synthesis, total chlorophyll degradation, ribonuclease activation and the decline in phosphoglycerokinase in senescing segments of *F. pratensis* leaves. Tissue treated with the L-isomer was indistinguishable from the water control. The present study confirms and extends these early observations.

Chlorophyll *a* and chl *b* were almost completely degraded in segments of Y *Lolium* incubated on water or L-MDMP for 6 d in the dark (Table 1). D-MDMP was highly effective in preventing loss of the pigments, superficially maintaining an unchanged presenescent greenness even in 6 d-senesced segments (Table 1, Fig. 2). Figure 3(a,b) also confirm the observation of Thomas (1976) and Thomas & Smart (1993) that D-MDMP is only partially effective in blocking the loss of total protein, and rubisco in particular. The staygreen mutation introgressed into *L. temulentum* from *F. pratensis* has been shown to have only a small stabilizing effect on rubisco protein (Thomas *et al.*, 1999) and function (Hauck *et al.*, 1997) during senescence. The response to D-MDMP of the

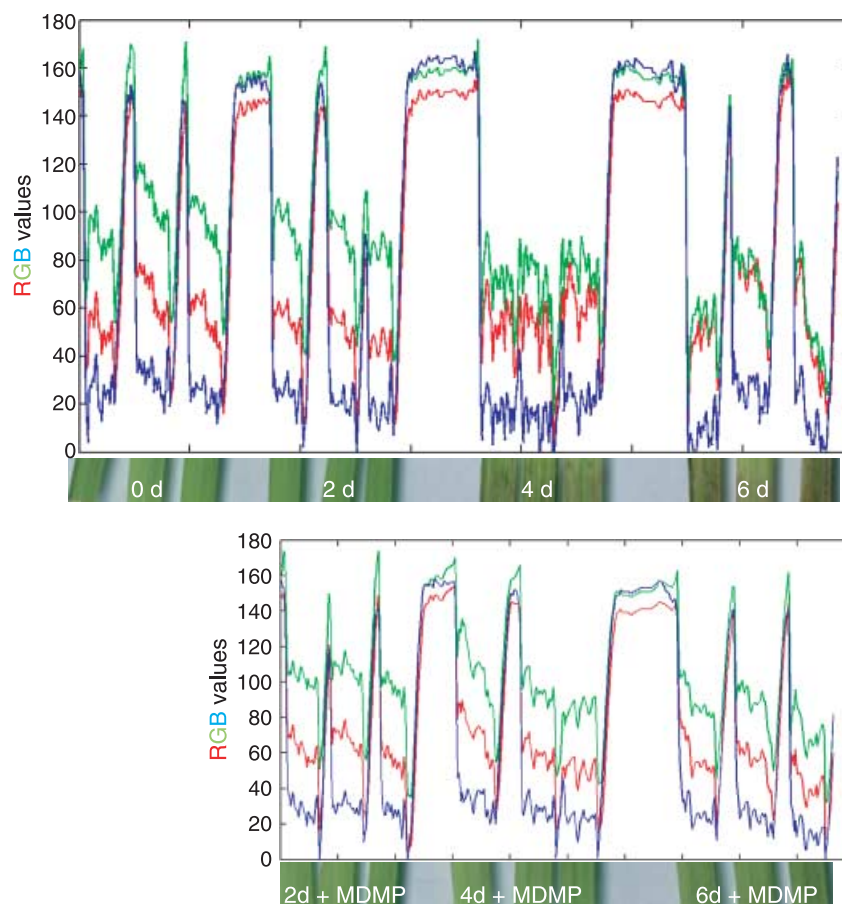


**Fig. 7** Profiles of red-green-blue (RGB) pixel values obtained by scanning JPEG images of G leaf segments treated with water or D-MDMP.

total protein and rubisco of the G genotype of *L. temulentum* is very close to that of Y, allowing for the stabilizing effect on (mostly pigment-binding) proteins of the chl retained by mutant segments (Fig. 3b,d). Despite many years of investigation, the biochemical basis and control of protein mobilization in senescing leaf cells is still incompletely understood (Hörtensteiner & Feller, 2002; Feller *et al.*, 2007). The present results indicate that different proteins may be degraded by different proteolytic pathways, some of which are newly made during senescence while others are constitutive or regulated post-translationally (Sullivan *et al.*, 2003; Hopkins *et al.*, 2007; Wingler, 2007).

#### Chlorophyll degradation in senescing leaf cells

The response of the chl of G segments to MDMP treatment raises questions concerning the mechanism of pigment degradation during senescence. Vicentini *et al.* (1995) observed that G *Festuca* has a deficiency in the activity of PaO, the enzyme responsible for opening the macrocycle of chl and destroying the green colour. Subsequently, it was shown that the staygreen introgression line of *L. temulentum* retains a basal level of PaO activity and accumulates essentially normal amounts of PaO protein during senescence (Roca *et al.*, 2004; Ougham *et al.*, in press). Armstead *et al.* (2006, 2007) cloned

the staygreen locus and showed it was a gene of unknown function with no similarity to PaO. The evidence points to a role in dismantling chlorophyll-protein complexes, with the indirect consequence of modulating PaO activity (Armstead *et al.*, 2006; Park *et al.*, 2007). The staygreen gene is not expressed before senescence is initiated and it is likely that D-MDMP and other protein synthesis inhibitors check yellowing by preventing the senescence-specific *de novo* synthesis of this critical protein. This cannot be the only point at which inhibitors act on chlorophyll metabolism in senescence, however. A consequence of the metabolic block at staygreen/PaO is that upstream intermediates in the pathway accumulate in senescing staygreen tissues (Thomas *et al.*, 1989; Roca *et al.*, 2004, Table 1). It was shown previously (Thomas *et al.*, 1989) that cycloheximide inhibits this accumulation. D-MDMP has a similar effect (Fig. 2). Since neither chlorophyllase nor the Mg-dechelating activity, which converts chl *a* to phaeophorbide *a*, is sensitive to inhibition of protein synthesis, the existence of another, as yet unidentified, component of the chl catabolism pathway (perhaps some kind of pigment transporter) is hypothesized (Matile *et al.*, 1999). On the other hand, Table 1 suggests a possible alternative source of inhibitor-sensitive phd accumulation in staygreen tissues. Chl *b* is comparatively unstable in the mutant, as the marked increase in *a* : *b* ratio

during senescence testifies. D-MDMP is highly effective in preventing chl *b* loss. It is well established that chl *b* is degraded by the PaO route after first being converted to phd *a* (Matile *et al.*, 1999). Scheumann *et al.* (1999) described a chl *b*-to-*a* conversion activity in barley that is up-regulated in senescence, and the gene for the corresponding reductase has recently been cloned (Kusaba *et al.*, 2007). If, as seems likely, this activation is sensitive to protein synthesis inhibition, it may explain phd accumulation in terms of *de novo* conversion of chl (or chld) *b* to chld *a*, followed by Mg dechelation. Chl *a*, by contrast, is much less labile than chl *b* in the mutant (Table 1). This may reflect differences in the accessibilities of chl *a* and *b* to components of the catabolic system invading the thylakoid membrane.

### Nondestructive analysis of pigment metabolism in senescing mesophyll cells

A direct sight imaging spectrograph has been used to record, at pixel resolution, visible differences in *L. temulentum* senescence genotypes and responses to MDMP treatment. The instrument generates large amounts of data. After appropriate corrections for background, illumination and spectrograph sensitivity, data complexity was reduced by carrying out PCA. The first five principal components accounted for more than 91% of the variance. Observations that behave similarly were grouped by plotting PC1 against PC2 (Fig. 4). The effect of introducing the *F. pratensis* G gene into the *L. temulentum* background is to change the trajectory of spectral reflectance through PC space (Fig. 4a). The large movements between days 4 and 6, and 6 and 8 in PC1/PC2 plots of G tissue demonstrate clearly that the mutation does not disable physiological processes leading to detectable spectral changes. After long incubations (6 d), both G and Y show a marked change in the direction of travel in PC data space. We believe that this is indicative of senescence being overtaken by programmed or pathological cell death. Blocking protein synthesis by treating with D-MDMP is effective in immobilizing the condition of the tissue at, or close to, the presenescent state (Fig. 4b), although some catabolic processes (e.g. Rubisco degradation) partially escape inhibition (Fig. 3). These observations reinforce the view that senescence is a combination of regulatory mechanisms acting at different points in the sequence of transcriptional, translational and post-translational events (Wingler, 2007; Jansson & Thomas, in press). Difference spectra (Fig. 6) give insights into the nature of the pigmentation changes occurring during senescence, and the compositional consequences of altered chlorophyll catabolism in the mutant. Note that the ordinate values are not directly comparable between Fig. 6(a) and (b) because data were autoscaled for plotting. The spectral properties of phd, which accumulates at the blockage point in the chlorophyll catabolism pathway in G (Roca *et al.*, 2004, Fig. 2), correspond to the reflectance signature of day 6 vs day 0 G. A blue shift of 10–15 nm is consistent with known differences in the properties of pigments

measured *in vivo* and *in vitro* (Röder *et al.*, 2000; Zucchelli *et al.*, 2002). MDMP treatment confirms that development of the presumptive phd signature *in vivo* is protein synthesis-dependent (Fig. 6b), as revealed by HPLC analysis of pigment extracts (Fig. 2). Corresponding changes in the balance between red and green reflectance are readily detected by analysis of RGB pixel values in photographic or scanned images (Figs 1, 7) and could be the basis of a simple high-throughput screening method.

### The senescing mesophyll cell – a suitable case for systems biology treatment

Mesophyll cell senescence has a number of features that make it a particularly appropriate subject for detailed molecular and physiological analysis. It occurs in post-mitotic, nongrowing tissue and so quantification of activities is not bedevilled by changing baselines. The cells in a given volume of mesophyll are well synchronized and the most important cellular and molecular events occurring in excised tissue incubated *in vitro* are qualitatively the same as those occurring in intact organs and plants (Ginsburg & Matile, 1993; Roca *et al.*, 2004). Senescence is self-reporting through pigmentation changes (Fig. 1) and, as shown here and in other studies using, for example, chlorophyll fluorescence (Wingler *et al.*, 2004), can be probed noninvasively to reveal the state of diagnostic metabolic pathways. Experimentally induced senescence is a terminal process of development expressed under conditions in which the environmental inputs that drive growth and biosynthesis can be excluded. Consequently, the important metabolic sequences are strongly one-way (catabolic) and individual reaction steps are effectively irreversible, avoiding the requirement for complex analyses of turnover and equilibrium kinetics. Even so, the senescence timeline can be readily run backwards with the appropriate treatments, and may in principle be shunted back and forth at will (Zavaleta-Mancera *et al.*, 1999a,b). The biochemistry of chlorophyll metabolism in senescing cells has become well understood in recent years (Kräutler & Hörtensteiner, 2006), most of the key genes have been isolated and there is a growing catalogue of mutants and knockouts in critical steps (Ougham *et al.*, in press). The present study describes observations of a mutant blocked at the macrocycle-opening step as a consequence of impairment in unpacking pigment-protein complexes (Armstead *et al.*, 2006). Other mutants – for example, *acd1*, *acd2* and *nyc1* – target other reactions in the catabolic sequence (Ougham *et al.*, in press). Precise chemical or pharmacological perturbation (in the present study we used a stereospecific protein synthesis inhibitor) can give direct information on biochemistry and gene expression in this system and suggests strongly that current interest in application of omics and systems biology techniques (Andersson *et al.*, 2004; Guo *et al.*, 2004; Buchanan-Wollaston *et al.*, 2005) is likely to pay off. Finally, mesophyll senescence survives scaling from the molecular through the physiological

to the agronomic and ecological, where it is demonstrably a primary determinant of high-level attributes such as adaptation, fitness and crop yield (Thomas, 1992; Thomas & Howarth, 2000; Thomas & Sadras, 2001; Munné-Bosch, 2007). For these practical reasons, as well as experimental tractability, there is a strong argument for including senescence amongst the priorities for the application of plant systems biology approaches.

## Acknowledgements

Research at IGER and Aberystwyth University on spectral imaging and multivariate analysis has been partially funded by the UK National Endowment for Science, Technology and the Arts, the Department for Environment, Food and Rural Affairs and the UK Biotechnology and Biological Sciences Research Council (BBSRC) Bioinformatics and E-science Program initiative. MR acknowledges support by the Ministerio de Ciencia y Tecnología (contract Juan de la Cierva). HT is the recipient of a Leverhulme Trust Emeritus Fellowship. The authors are grateful to Heather Ackroyd and Dan Harvey, a constant source of inspiration, creativity and new perspectives. IGER is sponsored by the BBSRC.

## References

- Andersson A, Keskitalo J, Sjödin A, Bhalerao R, Sterky F, Wissel K, Tandre K, Aspeborg H, Moyle R, Ohmiya Y *et al.* 2004. A transcriptional timetable of autumn senescence. *Genome Biology* 5: R2.
- Armstead I, Donnison I, Aubry S, Harper J, Hörtensteiner S, James C, Mani J, Moffet M, Ougham H, Roberts L *et al.* 2006. From crop to model to crop: identifying the genetic basis of the staygreen mutation in the *Lolium/Festuca* forage and amenity grasses. *New Phytologist* 172: 592–597.
- Armstead I, Donnison I, Aubry S, Harper J, Hörtensteiner S, James C, Mani J, Moffet M, Ougham H, Roberts L *et al.* 2007. Cross-species identification of Mendel's I locus. *Science* 315: 73.
- Baxter R, Knell VC, Somerville HJ, Swain HJ, Weeks DP. 1973. Effect of MDMP on protein synthesis in wheat and bacteria. *Nature New Biology* 243: 139–142.
- Bishop CM. 2006. *Pattern recognition and machine learning*. New York, NY, USA: Springer.
- Buchanan-Wollaston V, Page T, Harrison E, Breeze E, Lim PO, Nam HG, Lin J-F, Wu S-H, Swidzinski J, Ishizaki K *et al.* 2005. Comparative transcriptome analysis reveals significant differences in gene expression and signalling pathways between developmental and dark/starvation-induced senescence in *Arabidopsis*. *Plant Journal* 42: 567–585.
- Feller U, Anders I, Mae T. 2007. Rubiscolytics: fate of Rubisco after its enzymatic function in a cell is terminated. *Journal of Experimental Botany*, doi: 10.1093/jxb/erm242
- Gay AP, Hauck BD. 1994. Acclimation of *Lolium temulentum* to enhanced carbon dioxide concentration. *Journal of Experimental Botany* 45: 1133–1141.
- Ginsburg S, Matile P. 1993. Identification of catabolites of chlorophyll-porphyrin in senescent rape cotyledons. *Plant Physiology* 102: 521–527.
- Guo Y, Cai Z, Gan S. 2004. Transcriptome of *Arabidopsis* leaf senescence. *Plant, Cell & Environment* 27: 521–549.
- Hauck BD, Gay AP, Macduff JH, Griffiths CM, Thomas H. 1997. Leaf senescence in a nonyellowing mutant of *Festuca pratensis*: implications of the stay-green mutation for photosynthesis, growth and nutrition. *Plant, Cell & Environment* 20: 1007–1018.
- Hopkins M, Taylor C, Liu Z, Ma F, McNamara L, Wang T-W, Thompson JE. 2007. Regulation and execution of molecular disassembly and catabolism during senescence. *New Phytologist* 175: 201–214.
- Hörtensteiner S, Feller U. 2002. Nitrogen metabolism and remobilization during senescence. *Journal of Experimental Botany* 53: 927–937.
- Hotelling H. 1933. Analysis of complex statistical variables into principal components. *Journal of Educational Psychology* 24: 417–441.
- Jansson S, Thomas H. (in press). Senescence – developmental program or timetable? *New Phytologist*.
- Kräutler B, Hörtensteiner S. 2006. Chlorophyll catabolites and the biochemistry of chlorophyll breakdown. In: Grimm B, Porra R, Rüdiger W, Scheer H, eds. *Chlorophylls and bacteriochlorophylls: biochemistry, biophysics, functions and applications*. Dordrecht, the Netherlands: Springer, 237–260.
- Kusaba M, Ito H, Morita R, Iida S, Sato Y, Fujimoto M, Kawasaki S, Tanaka R, Hirochika H, Nishimura M *et al.* 2007. Rice NONYELLOW COLORING1 is involved in light-harvesting complex II and grana degradation during leaf senescence. *Plant Cell* 19: 1362–1375.
- Laemmli UK. 1970. Cleavage of structural proteins during the assembly of the head of bacteriophage T4. *Nature* 227: 681–685.
- Langmeier M, Ginsburg S, Matile P. 1993. Chlorophyll breakdown in senescent leaves – demonstration of Mg-dechelataase activity. *Physiologia Plantarum* 89: 347–353.
- Lowry OH, Roseborough NJ, Farr AL, Randall RJ. 1951. Protein measurement with the Folin phenol reagent. *Journal of Biological Chemistry* 193: 265–275.
- Manly BFJ. 2000. *Multivariate statistical methods a primer*. Boca Raton, FL, USA: CRC.
- Matile P, Hörtensteiner S, Thomas H. 1999. Chlorophyll degradation. *Annual Review of Plant Physiology and Plant Molecular Biology* 50: 67–95.
- Merzlyak MN, Gitelson AA, Chivkunova OB, Rakitin VY. 1999. Nondestructive optical detection of pigment changes during leaf senescence and fruit ripening. *Physiologia Plantarum* 106: 135–141.
- Mitchell TM. 1997. *Machine learning*. New York, NY, USA: McGraw-Hill.
- Munné-Bosch S. 2007. Aging in perennials. *Critical Reviews in Plant Sciences* 26: 123–138.
- Naes T, Isaksson T, Fearn T, Davies T. 2004. *Multivariate calibration and classification*. Chichester, UK: NIR publications.
- Ougham H, Hörtensteiner S, Armstead I, Donnison I, King I, Thomas H, Mur L. (in press). The control of chlorophyll catabolism and the status of yellowing as a biomarker of leaf senescence. *Plant Biology*.
- Park S-Y, Yu J-W, Park J-S, Li J, Yoo S-C, Lee N-Y, Lee S-K, Jeong S-W, Seo HS, Koh H-J *et al.* 2007. The senescence-induced staygreen protein regulates chlorophyll degradation. *Plant Cell* 19: 1649–1664.
- Richardson AD, Duigan SP, Berlyn GP. 2002. An evaluation of noninvasive methods to estimate foliar chlorophyll content. *New Phytologist* 153: 185–194.
- Roca M, James C, Pružinská A, Hörtensteiner S, Thomas H, Ougham H. 2004. Analysis of the chlorophyll catabolism pathway in leaves of an introgression senescence mutant of *Lolium temulentum*. *Phytochemistry* 65: 1231–1238.
- Röder B, Hanke TH, Oelckers ST, Hackborth ST, Symietz CH. 2000. Photophysical properties of pheophorbide *a* in solution and in model membrane systems. *Journal of Porphyrins and Phthalocyanines* 4: 37–44.
- Scheumann V, Schoch S, Rüdiger W. 1999. Chlorophyll *b* reduction during senescence of barley seedlings. *Planta* 209: 364–370.
- Siefermann-Harms D. 1987. The light-harvesting and protective functions of carotenoids in photosynthetic membranes. *Physiologia Plantarum* 69: 561–568.
- Sims DA, Gamon JA. 2002. Relationships between leaf pigment content and spectral reflectance across a wide range of species, leaf structures and developmental stages. *Remote Sensing of Environment* 81: 337–354.

- Sullivan JA, Shirasu K, Deng XW. 2003. The diverse roles of ubiquitin and the 26S proteasome in the life of plants. *Nature Reviews Genetics* 4: 948–958.
- Tanaka A, Tanaka R. 2006. Chlorophyll metabolism. *Current Opinion in Plant Biology* 9: 248–255.
- Thomas H. 1976. Delayed senescence in leaves treated with the protein synthesis inhibitor MDMP. *Plant Science Letters* 6: 369–377.
- Thomas H. 1992. Canopy survival. In: Baker N, Thomas H, eds. *Crop photosynthesis: spatial and temporal determinants*. Amsterdam, the Netherlands: Elsevier, 11–41.
- Thomas H, Bortlik K, Rentsch D, Schellenberg M, Matile PH. 1989. Catabolism of chlorophyll in vivo: significance of polar chlorophyll catabolites in a nonyellowing senescence mutant of *Festuca pratensis* Huds. *New Phytologist* 111: 3–8.
- Thomas H, Howarth CJ. 2000. Five ways to stay green. *Journal of Experimental Botany* 51: 329–337.
- Thomas H, Morgan WG, Thomas AM, Ougham HJ. 1999. Expression of the stay-green character introgressed into *Lolium temulentum* Ceres from a senescence mutant of *Festuca pratensis*. *Theoretical and Applied Genetics* 99: 92–99.
- Thomas H, Ougham H, Hörtensteiner S. 2001. Recent advances in the cell biology of chlorophyll catabolism. *Advances in Botanical Research* 35: 1–52.
- Thomas H, Ougham HJ, Wagstaff C, Stead AJ. 2003. Defining senescence and death. *Journal of Experimental Botany* 54: 1127–1132.
- Thomas H, Sadras VO. 2001. The capture and gratuitous disposal of resources by plants. *Functional Ecology* 15: 3–12.
- Thomas H, Smart CM. 1993. Crops that stay green. *Annals of Applied Biology* 123: 193–219.
- Thomas H, Stoddart JL. 1980. Leaf senescence. *Annual Review of Plant Physiology* 31: 83–111.
- Vicentini F, Hoertensteiner S, Schellenberg M, Thomas H, Matile PH. 1995. Chlorophyll breakdown in senescent leaves: identification of the biochemical lesion in a stay-green genotype of *Festuca Pratensis*. *New Phytologist* 129: 247–252.
- Wingler A. 2007. Transcriptional or posttranscriptional regulation – how does a plant know when to senesce? *New Phytologist* 175: 1–4.
- Wingler A, Marès M, Pourtau N. 2004. Spatial patterns and metabolic regulation of photosynthetic parameters during leaf senescence. *New Phytologist* 161: 781–789.
- Witten IH, Frank E. 2005. *Data mining*. San Francisco, CA, USA: Morgan Kaufman.
- Zarco-Tejada PJ, Berjón A, López-Lozano R, Miller JR, Martín P, Cachorro V, González MR, de Frutos A. 2005. Assessing vineyard condition with hyperspectral indices: Leaf and canopy reflectance simulation in a row structured Discontinuous canopy. *Remote Sensing of Environment* 99: 271–287.
- Zavaleta-Mancera HA, Franklin KA, Ougham HJ, Thomas H, Scott IM. 1999a. Regreening of senescent *Nicotiana* leaves. I. Reappearance of NADPH-protochlorophyllide oxidoreductase and light-harvesting chlorophyll a/b-binding protein. *Journal of Experimental Botany* 50: 1677–1682.
- Zavaleta-Mancera HA, Thomas BJ, Thomas H, Scott IM. 1999b. Regreening of senescent *Nicotiana* leaves. II. Redifferentiation of plastids. *Journal of Experimental Botany* 340: 1683–1689.
- Zucchelli G, Jennings RC, Garlaschi FM, Cinque G, Bassi R, Cremones O. 2002. The calculated in vitro and in vivo chlorophyll a absorption bandshape. *Biophysical Journal* 82: 378–390.

## Supplementary Material

The following supplementary material is available for this article online:

**Fig. S1** Reflectance data from which the difference spectra in Fig. 6(b) were generated.

This material is available as part of the online article from:

<http://www.blackwell-synergy.com/doi/abs/10.1111/j.1469-8137.2008.02412.x>

(This link will take you to the article abstract).

Please note: Blackwell Publishing are not responsible for the content or functionality of any supplementary materials supplied by the authors. Any queries (other than missing material) should be directed to the journal at *New Phytologist* Central Office.



## About *New Phytologist*

- *New Phytologist* is owned by a non-profit-making **charitable trust** dedicated to the promotion of plant science, facilitating projects from symposia to open access for our Tansley reviews. Complete information is available at [www.newphytologist.org](http://www.newphytologist.org).
- Regular papers, Letters, Research reviews, Rapid reports and both Modelling/Theory and Methods papers are encouraged. We are committed to rapid processing, from online submission through to publication 'as-ready' via *OnlineEarly* – our average submission to decision time is just 29 days. Online-only colour is **free**, and essential print colour costs will be met if necessary. We also provide 25 offprints as well as a PDF for each article.
- For online summaries and ToC alerts, go to the website and click on 'Journal online'. You can take out a **personal subscription** to the journal for a fraction of the institutional price. Rates start at £135 in Europe/\$251 in the USA & Canada for the online edition (click on 'Subscribe' at the website).
- If you have any questions, do get in touch with Central Office ([newphytol@lancaster.ac.uk](mailto:newphytol@lancaster.ac.uk); tel +44 1524 594691) or, for a local contact in North America, the US Office ([newphytol@ornl.gov](mailto:newphytol@ornl.gov); tel +1 865 576 5261).